Published OnlineFirst September 23, 2016; DOI: 10.1158/1078-0432.CCR-16-0620

Biology of Human Tumors

Clinical Cancer Research

Selective Targeting of Cyclin E1-Amplified High-Grade Serous Ovarian Cancer by Cyclin-Dependent Kinase 2 and AKT Inhibition

George Au-Yeung[1,2], Franziska Lang[1], Walid J. Azar[1], Chris Mitchell[1], Kate E. Jarman[3], Kurt Lackovic[3,4], Diar Aziz[5], Carleen Cullinane[1,6], Richard B. Pearson[1,2,7], Linda Mileshkin[2,8], Danny Rischin[2,8], Alison M. Karst[9], Ronny Drapkin[10], Dariush Etemadmoghadam[1,2,5], and David D.L. Bowtell[1,2,7,11]

Abstract

Purpose: Cyclin E1 (*CCNE1*) amplification is associated with primary treatment resistance and poor outcome in high-grade serous ovarian cancer (HGSC). Here, we explore approaches to target *CCNE1*-amplified cancers and potential strategies to overcome resistance to targeted agents.

Experimental Design: To examine dependency on *CDK2* in *CCNE1*-amplified HGSC, we utilized siRNA and conditional shRNA gene suppression, and chemical inhibition using dinaciclib, a small-molecule CDK2 inhibitor. High-throughput compound screening was used to identify selective synergistic drug combinations, as well as combinations that may overcome drug resistance. An observed relationship between *CCNE1* and the AKT pathway was further explored in genomic data from primary tumors, and functional studies in fallopian tube secretory cells.

Results: We validate *CDK2* as a therapeutic target by demonstrating selective sensitivity to gene suppression. However, we found that dinaciclib did not trigger amplicon-dependent sensitivity in a panel of HGSC cell lines. A high-throughput compound screen identified synergistic combinations in *CCNE1*-amplified HGSC, including dinaciclib and AKT inhibitors. Analysis of genomic data from TCGA demonstrated coamplification of *CCNE1* and *AKT2*. Overexpression of Cyclin E1 and AKT isoforms, in addition to mutant *TP53*, imparted malignant characteristics in untransformed fallopian tube secretory cells, the dominant site of origin of HGSC.

Conclusions: These findings suggest a specific dependency of *CCNE1*-amplified tumors for AKT activity, and point to a novel combination of dinaciclib and AKT inhibitors that may selectively target patients with *CCNE1*-amplified HGSC. *Clin Cancer Res; 23(7); 1862–74. ©2016 AACR.*

Introduction

Targeted therapies have changed the management of many cancers types, resulting in significant improvements in clinical response rates and survival (1). However, while the antiangiogenic mAb bevacizumab (2, 3) and the PARP inhibitor olaparib (4, 5) have entered care in high-grade serous ovarian cancer (HGSC) recently, the development of targeted therapy to this disease has been relatively slow.

HGSCs are characterized by ubiquitous *TP53* mutations, genomic instability, and widespread copy number alterations, with relatively infrequent somatic point mutations of driver genes (6, 7). Structural aberration also contributes to loss of tumor suppressors such as *RB1* and *NF1* by gene breakage (8). Defects in the homologous recombination repair (HR) pathway are present in approximately 50% of HGSCs, primarily associated with germline and somatic mutations in *BRCA1*, *BRCA2*, and associated proteins (7). HR deficiency imparts platinum sensitivity in HGSC, and provides the basis for the use of PARP inhibitors that target compensatory DNA repair pathways (4, 9). Of HGSC with intact HR, amplification of *CCNE1*, which encodes the cell-cycle regulator cyclin E1, is the best characterized driver. *CCNE1* amplification or gain occurs in 20% of all HGSC tumors and is associated with primary treatment resistance and reduced overall survival in HGSC (10, 11). Patients whose tumors have *CCNE1*

[1]Division of Cancer Research, Peter MacCallum Cancer Centre, Melbourne, Victoria, Australia. [2]Sir Peter MacCallum Department of Medical Oncology, University of Melbourne, Parkville, Victoria, Australia. [3]Walter and Eliza Hall Institute of Medical Research, Parkville, Victoria, Australia. [4]Department of Medical Biology, University of Melbourne, Parkville, Victoria, Australia. [5]Department of Pathology, University of Melbourne, Parkville, Victoria, Australia. [6]Translational Research Program, Peter MacCallum Cancer Centre, East Melbourne, Victoria, Australia. [7]Department of Biochemistry and Molecular Biology, University of Melbourne, Parkville, Victoria, Australia. [8]Department of Medical Oncology, Peter MacCallum Cancer Centre, East Melbourne, Victoria, Australia. [9]Department of Medical Oncology, Dana Farber Cancer Institute, Boston, Massachusetts. [10]Division of Gynecologic Oncology, Department of Obstetrics and Gynecology, Penn Ovarian Cancer Research Center, University of Pennsylvania Perelman School of Medicine, Philadelphia, Pennsylvania. [11]Kinghorn Cancer Centre, Garvan Institute for Medical Research, Darlinghurst, New South Wales, Australia.

Note: Supplementary data for this article are available at Clinical Cancer Research Online (http://clincancerres.aacrjournals.org/).

D. Etemadmoghadam and D.D.L. Bowtell contributed equally to this article.

Corresponding Author: David D.L. Bowtell, Peter MacCallum Cancer Centre, Locked Bag I, A'Beckett Street, Melbourne, Victoria 8006, Australia. Phone: 613-8559-7108; E-mail: david.bowtell@petermac.org

doi: 10.1158/1078-0432.CCR-16-0620

Published OnlineFirst September 23, 2016; DOI: 10.1158/1078-0432.CCR-16-0620

Translational Relevance

High-grade serous ovarian cancer (HGSC) patients with Cyclin E1 (*CCNE1*) amplification represent a group with high unmet clinical need. Novel therapies are needed to improve outcomes in these patients, given that *CCNE1*-amplified tumors are unlikely to respond to chemotherapy or PARP inhibitors, and are associated with poor overall survival. Here, we validate *CDK2* as a selective target for *CCNE1*-amplified cell lines. We performed a high-throughput compound screen and identified a number of potential therapeutic combinations. We focused on dinaciclib and AKT inhibitors, and demonstrate selective and potent activity in *CCNE1*-amplified HGSC. We further show cooperation between *CCNE1* and *AKT*, both in genomic data from TCGA and functionally in fallopian tube secretory cells. This study demonstrates approaches to target an important subset of solid cancers, and for the first time provides evidence to support the design of a rational clinical trial that targets *CCNE1*-amplified HGSC.

amplification represent a group with unmet clinical need, as they are unlikely to benefit from PARP inhibitors by virtue of the mutual exclusivity of *CCNE1* amplification and *BRCA1/2* mutation (7, 12), and are less likely to respond to platinum agents.

In recent preclinical studies, we have shown a dependency on CDK2 (13) and HR activity (12) in *CCNE1*-amplified cell lines. Although targeted agents have been effective in the clinical setting across many cancers, the emergence of acquired resistance is common (14). Indeed, we reported *in vitro* resistance to CDK2 inhibitors through selection of a polyploid population in the *CCNE1*-amplified cell line OVCAR3 (13). Rational drug combinations are a potential strategy to prevent resistance (15), and may also facilitate improvements in the therapeutic window by reducing the doses of drugs required to achieve efficacy, resulting in fewer side effects (16). We therefore used a high-throughput drug screen to identify drug combinations that synergize with the CDK2 inhibitor dinaciclib (17) to selectively target *CCNE1*-amplified HGSC, and to overcome resistance in a cell line that has acquired resistance to CDK inhibitors *in vitro* (13). We identified several synergistic combinations, including dinaciclib and AKT inhibitors, and found that that this synergy extended more generally to *CCNE1*-amplified HGSC cell lines. Our results suggest targeting CDK2 and the AKT pathway may be an important approach to the clinical management of *CCNE1*-amplified HGSC.

Materials and Methods

Ethics statement

All animal experiments were approved by the Peter MacCallum Cancer Centre Animal Experimentation Ethics Committee and conducted in accordance with the National Health and Medical Research Council Australian Code of Practice for the Care and Use of Animals for Scientific Purposes.

Cell lines

Ovarian cancer cell lines were obtained from the National Cancer Institute Repository, actively passaged for less than 6 months, and authenticated using short-tandem repeat markers to confirm their identity against the Cancer Genome Project database (Wellcome Trust Sanger Institute, Cambridgeshire, United Kingdom) before use in experiments. Cells were maintained at 37°C and 5% CO_2 (v/v), and cultured in RPMI1640 media containing 10% (v/v) FCS and 1% penicillin/streptomycin. Transfection and drug sensitivity assays were performed in the absence of antibiotics. Cell lines resistant to dinaciclib were generated utilizing methods as described previously (13). Briefly, OVCAR3 cells were plated in 6-well plates and treated with dinaciclib at the IC_{50} dose for two 72-hour periods (media removed and fresh drug added). Surviving cells were allowed to repopulate for 96 hours and the process repeated once. Remaining cells were cultured in media or in the presence of drug, and regularly monitored for sensitivity to dinaciclib. Six independent cell lines were generated in this fashion, and designated OVCAR3-RD1 to -RD6.

Short hairpin–mediated *CDK2* knockdown

Short hairpin–mediated knockdown of *CDK2* was performed by cloning CDK2-specific shRNA into a lentiviral tetracycline-inducible expression vector containing the optimized miR-E backbone (18). The modified lentiviral vector pRRL-T3G-TurboGFP-miRE-PGK-mCherry-IRES-rTA3 (also referred to as LT3GECIR) system includes a red (mCherry) fluorescent marker for transduction and a green (turboGFP) fluorescent marker for induction. Five CDK2-specific shRNA constructs were cloned into this system (see Supplementary Table S1 for sequences). For lentiviral production, HEK293T cells were transfected with plasmid DNA combined with the Lenti-X packaging system (Clontech Laboratories). Transfection, production of lentiviral particles, and transduction of target cells was performed as described by the manufacturer's protocol. Doxycycline was used to induce shRNA expression, and transfection efficiency was validated by flow cytometry (FACS), and knockdown of individual hairpins by RT-PCR and Western blot analysis. The most efficient shRNA construct was taken forward for *in vitro* and *in vivo* experiments.

For *in vivo* experiments, xenograft tumors from transduced cells were generated as described below. Once tumors reached 100 mm^3, mice were randomized into two groups to receive either normal food and water or doxycycline food and water (2 mg/mL in 2% sucrose) as a means of reliable induction of shRNA expression. Tumors were subsequently monitored as described below.

Cyclin E1 and AKT overexpression in Fallopian tube secretory epithelial cells

The immortalized fallopian tube secretory epithelial cell (FTSEC) line FT282 was obtained from Ronny Drapkin (University of Pennsylvania, Philadelphia, PA; ref. 19). Derivative cell lines were generated using pMSCV-mCherry-(empty) and pMSCV-mCherry-*CCNE1*, encoding full-length *CCNE1*. Additional cell lines were generated with pMSCV-GFP-myr-AKT1, pMSCV-GFP-myr-AKT2, and pMSCV-GFP-myr-AKT3, encoding the three different isoforms of myr-AKT (20). Plasmids were validated by sequencing, and expression of *CCNE1*, *AKT1*, *AKT2*, and *AKT3* was validated by quantitative real-time PCR and Western blotting. Primer sequences are listed in Supplementary Table S2.

High-throughput compound screen

The compound library consisted of 73 targeted agents, 71 epigenetic agents, 208 kinase inhibitors, and 3,707 known drugs

Published OnlineFirst September 23, 2016; DOI: 10.1158/1078-0432.CCR-16-0620

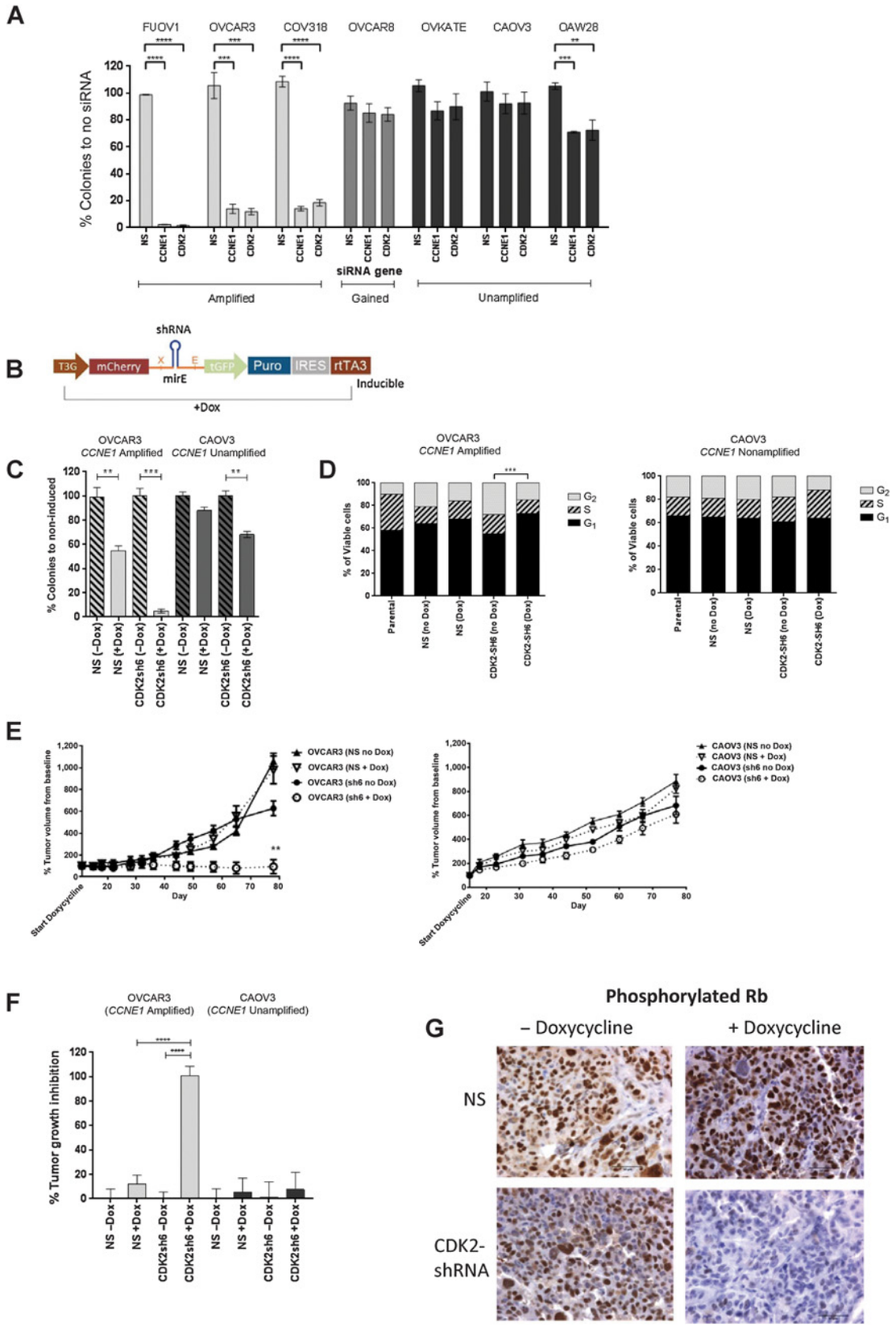

Published OnlineFirst September 23, 2016; DOI: 10.1158/1078-0432.CCR-16-0620

(21). All agents were dissolved in DMSO, and diluted to concentrations from 0.01 to 10 μmol/L. For targeted agents, epigenetic agents and kinase inhibitors, the primary screen was conducted using 11 concentrations; for the known drug library three concentrations were used. Compounds were dispensed into 384-well drug stock plates and stored at −20°C. Stock plates for dinaciclib at a fixed dose concentration (EC_{30}) were prepared using a multichannel pipette before each assay.

Early passage cells were deposited into 384-well microtiter plates at 750–1,500 cells per well using a multidrop dispenser (Thermo Scientific) in 40 μL of media. Cells were allowed to adhere overnight. A MiniTrak IX (PerkinElmer Life Sciences) automated robotic platform was used to dispense compounds into assay plates. Compounds were added directly to assay plates using a 384, hydrophobic slotted pintool (VP Scientific) calibrated to dispense 0.1 μL of DMSO compound solution. DMSO (0.1%) was used as negative control. Cells were exposed to drug for 48 hours, and cell viability measured using the CellTiter-Glo Luminescent Assay (Promega) and the EnVision Multilabel Plate Reader (PerkinElmer). Average viability was normalized to DMSO control wells, and EC_{50} dose was approximated by fitting a four-parameter dose–response curve using XLfit (IDBS).

Xenograft studies

Estrogen pellets were implanted subcutaneously into 4- to 6-week-old female NOD/SCID mice to facilitate the growth of xenografted cells. The pellet was implanted 3 days before injection of cells. Cell lines were grown *in vitro*, washed twice with PBS, and resuspended in 50% Matrigel (BD Biosciences) in PBS. Mice were injected subcutaneously with 5×10^6 cells in 100 μL, and monitored at least twice weekly. Tumor volume was calculated using the equation: volume = $(\text{width})^2 \times \text{length}/2$. When tumors reached 100 to 150 mm^3, mice were randomized into groups of five for treatment with vehicle alone or drug. Dinaciclib was prepared fresh before injection in 20% (w/v) hydroxypropyl-beta-cyclodextrin (Cyclodextrin Technologies Development, Inc.) and mice dosed twice weekly as a single agent via intraperitoneal injection. MK-2206 was reconstituted in 30% (w/v) Captisol (Ligand Technology) and dosed at 60 mg/kg three times per week as a single agent via oral gavage. For combination studies, MTDs of dinaciclib 20 mg/kg and MK-2206 60 mg/kg were dosed three times per week. All mice were monitored daily following drug dosing. Tumors were harvested at specific time points for biomarker analysis or at study endpoint, with half snap frozen in liquid nitrogen and half fixed in formalin and paraffin embedded for IHC. Percentage tumor growth inhibition (TGI) was calculated as $100 \times (1-\Delta T/\Delta C)$ where ΔC and ΔT were determined by subtracting the mean tumor volume (in the vehicle control and treated groups, respectively) on day 1 of treatment, from the mean tumor volume on each day of assessment. Statistical analyses were performed using GraphPad Prism Version 6.0 (GraphPad) with ANOVA followed by Dunnett *post hoc* test to compare the tumor growth between treatment groups.

CCNE1 and *AKT* status in primary ovarian tumor samples

Genomic alterations identified in *CCNE1* and genes involved in the PI3K–AKT–mTOR pathway were obtained from The Cancer Genome Atlas (TCGA) cBioPortal (22, 23). All available data as of March 2015 were analyzed, comprising 316 primary ovarian serous cystadenocarcinoma samples (7).

shRNA screen data

Data from the Project Achilles was obtained to evaluate the interaction between *CCNE1*-amplified ovarian cancer cell lines and genes in the AKT pathway (24). Cell line copy number data were obtained from the Cancer Cell Line Encyclopedia (25). Only cell lines known to resemble HGSC according to their genomic characteristics (26) were used in the analysis ($N = 14$, see Supplementary Table S3). Cell lines with a $\log_2$ copy number ratio > 0.3 over the *CCNE1* locus were designated as amplified ($n = 9$) and cell lines with a $\log_2$ copy number ratio < 0 were designated as unamplified ($n = 5$). Cell lines with *CCNE1* gene expression greater than the median +1 SD ($n = 9$) were defined as *CCNE1*-high expression, whereas cell lines with *CCNE1* gene expression less than median ($n = 5$) were defined as *CCNE1*-low expression.

Additional methods for gene suppression studies, Western blot analysis, IHC, flow cytometry and drug sensitivity, clonogenic, proliferation, and anchorage-independent growth assays can be found in Supplementary Methods.

Results

CCNE1-amplified HGSC cells are selectively sensitive to *CDK2* knockdown

We previously demonstrated in a limited number of cell lines that *CCNE1*-amplified HGSC cell lines are selectively sensitive to

Figure 1.

CDK2 knockdown via siRNA and shRNA *in vitro* and *in vivo* results in selective reduction in clonogenic survival and tumor growth arrest in *CCNE1*-amplified HGSC. **A,** Clonogenic survival after transfection with *CCNE1* and *CDK2* siRNAs in panel of HGSC cell lines. Average percentage of discrete colonies formed after 7 to 10 days relative to no siRNA controls shown ($n = 3$). Error bars, SEM. Statistical significance (*t* test) calculated by comparison with nonsilencing (NS) siRNA in the same cell line. **, $P < 0.01$, ***, $P < 0.001$, ****, $P < 0.0001$. **B,** Schematic of conditional LT3GECIR lentiviral vector showing inducible transcripts produced by vector. **C,** Clonogenic survival after induction of a nonspecific or CDK2-targeting shRNA in OVCAR3 (*CCNE1*-amplified) and CAOV3 (*CCNE1*-unamplified). The average percentage of discrete colonies formed after 7 to 10 days relative to no induction shown ($n = 3$). Statistical significance (*t* test) calculated by comparison with noninduced (−Dox) in the same cell line; **, $P < 0.01$, ***, $P < 0.001$. **D,** Cell-cycle analysis following CDK2 knockdown with inducible shRNA. Proportion of cells in G_1, S, or G_2 phase for propidium iodide (PI)-stained cells analyzed by flow cytometry 72 hours after induction with doxycycline. Mean of three independently performed experiments shown. Statistical significance (*t* test) calculated by comparison with noninduced (−Dox) in the same cell line. ***, $P < 0.001$. **E,** Mean percentage change in tumor volume ± SEM following induction of a nonspecific (NS) or CDK2 (sh6) shRNA in subcutaneous xenograft tumors grown in immunocompromised mice, generated from OVCAR3 and CAOV3. Induced and noninduced groups as marked, $n = 5$ per group. **, $P < 0.001$, unpaired *t* test comparison of mean percentage tumor volume change. **F,** Percentage tumor growth inhibition following induction of nonspecific (NS) or CDK2 (sh6) shRNA with doxycycline. Bars, mean ± SEM, $n = 5$ mice per group. Statistical analysis performed with ANOVA followed by Dunnett *post hoc* test to compare the percentage tumor growth inhibition between the treatment groups. ****, $P < 0.0001$. **G,** IHC assessment of phospho-Rb with or without doxycycline treatment in OVCAR3 xenograft tumor.

Published OnlineFirst September 23, 2016; DOI: 10.1158/1078-0432.CCR-16-0620

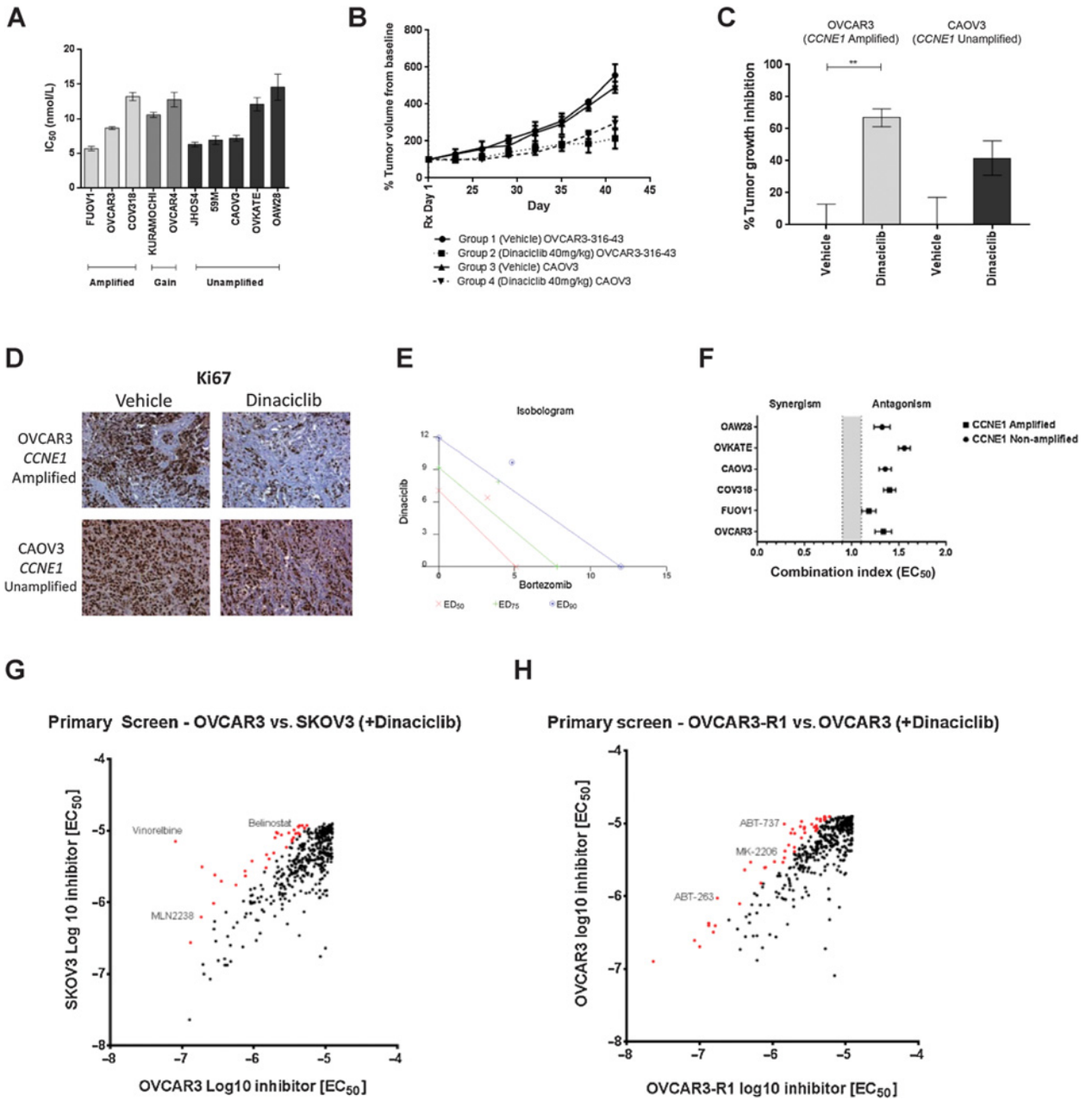

Figure 2.

CDK inhibitor dinaciclib results in modest tumor growth inhibition *in vivo* but is not synergistic in combination with bortezomib *in vitro*. **A,** Mean IC_{50} values for a panel of HGSC cell lines treated with dinaciclib generated from dose–response curves following standard MTS cell proliferation assays. Error bars, SEM, $n = 3$ experiments. **B,** *In vivo* effects of dinaciclib. Immunocompromised mice bearing OVCAR3 (*CCNE1*-amplified) or CAOV3 (*CCNE1*-unamplified) tumor xenografts were treated with vehicle or drug as described in Materials and Methods. Plots represent mean tumor volume change from baseline ± SEM, $n = 5$ mice per group. **C,** The percentage tumor growth inhibition following 21 days of treatment with vehicle or dinaciclib. Bars represent mean ± SEM, $n = 5$ mice per group. Statistical analysis performed with ANOVA followed by Dunnett *post hoc* test to compare the percentage tumor growth inhibition between the treatment groups. **, $P < 0.01$. **D,** Immunohistochemical analysis of Ki67 expression in OVCAR3 and CAOV3 tumor xenograft harvested 24 hours after dose of vehicle or dinaciclib. **E,** Formal assessment of synergy between dinaciclib and bortezomib using Chou–Talalay Isobologram analysis. Figures are generated with CalcuSyn 2.0. Data are normalized, with connecting line at X and Y corresponding to combination index = 1, representing line of additivity. Data points above the line are antagonistic, along or near the line are additive and points below the line are synergistic. **F,** Combination indexes for a panel of HGSC cell lines tested against dinaciclib in combination with bortezomib. Values represent mean ± SEM, $n = 3$. **G–H,** Scatter plots showing EC_{50} values for library compounds in combination with dinaciclib from primary screen for the comparison between *CCNE1*-amplified and unamplified (**G**) and resistant versus parental (**H**). Data points in red represent compounds taken forward for secondary screen.

Published OnlineFirst September 23, 2016; DOI: 10.1158/1078-0432.CCR-16-0620

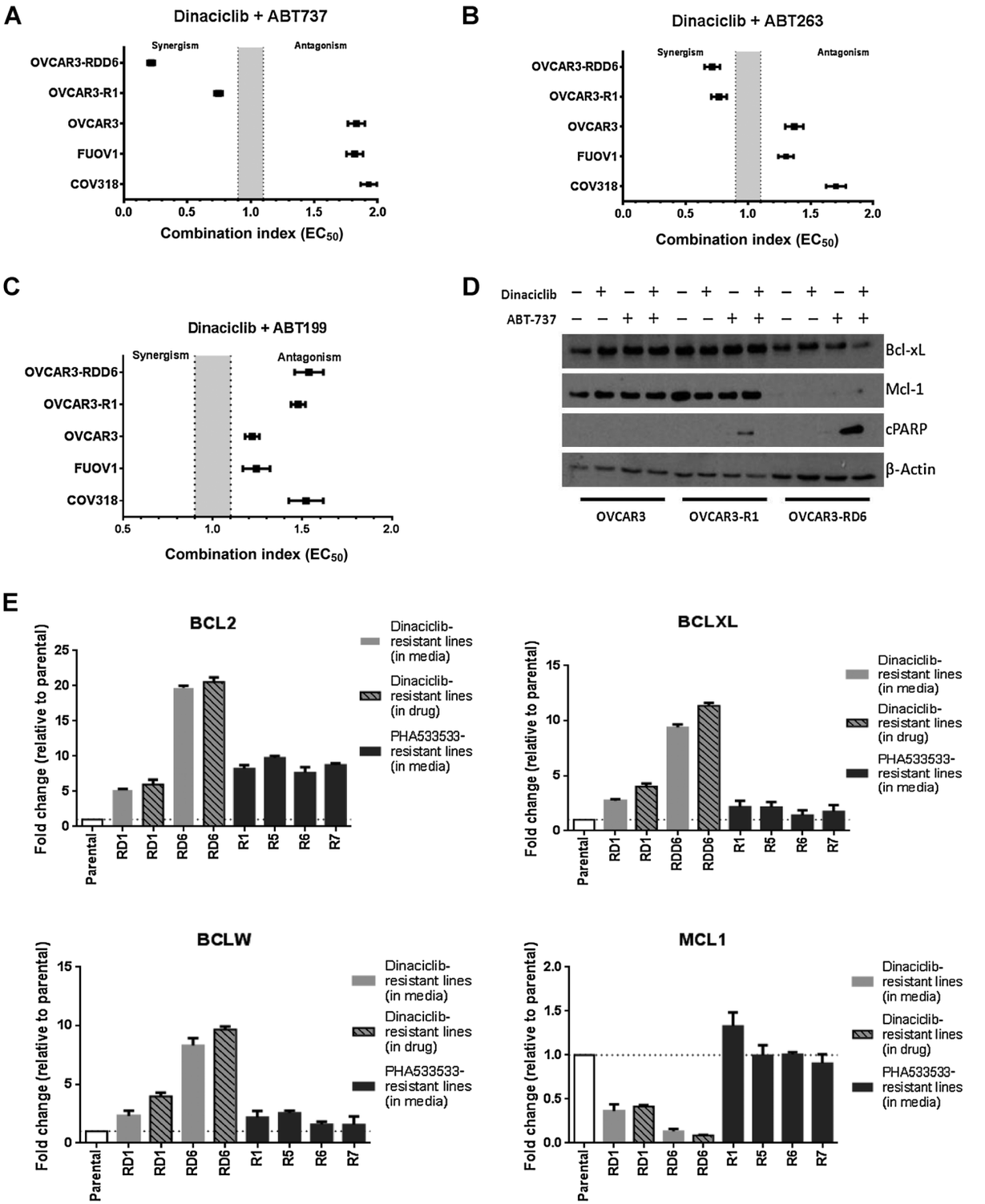

Figure 3.

Dinaciclib in combination with nonselective BH3 mimetics are synergistic in CDK inhibitor–resistant cell lines. Combination indexes for parental and CDK inhibitor–resistant cell lines tested against dinaciclib in combination with ABT-737 (**A**), ABT-263 (**B**), ABT-199 (**C**). Values represent mean ± SEM, $n = 3$. **D,** Western blot analysis demonstrating protein expression of Bcl-XL, Mcl-1, and PARP cleavage products in OVCAR3 parental and CDK inhibitor–resistant cell lines after treatment with dinaciclib and ABT-737. **E,** Expression of antiapoptotic proteins as assessed by quantitative real-time PCR. R-lines signify cell lines resistant to PHA533533. RD lines signify cell lines resistant to dinaciclib. Bars represent mean ± SEM, $n = 3$.

Published OnlineFirst September 23, 2016; DOI: 10.1158/1078-0432.CCR-16-0620

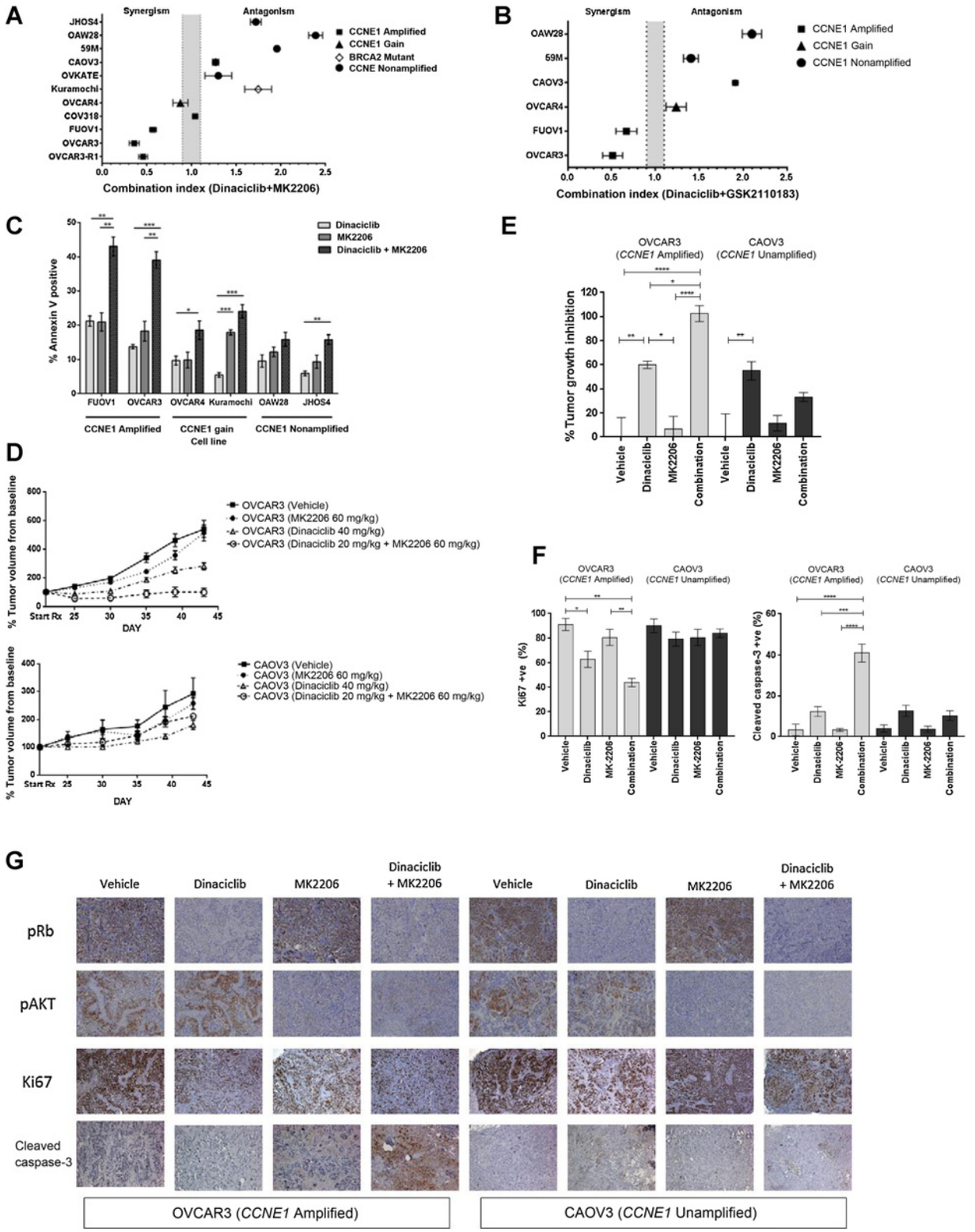

Figure 4.

Dinaciclib in combination with two AKT inhibitors are synergistic *in vitro* and *in vivo* models of *CCNE1*-amplified HGSC. Combination indexes for a panel of HGSC cell lines tested against dinaciclib in combination with MK-2206 (**A**) and GSK2110183 (**B**). Values represent mean ± SEM, (*Continued on the following page.*)

Published OnlineFirst September 23, 2016; DOI: 10.1158/1078-0432.CCR-16-0620

CCNE1 and *CDK2* knockdown mediated by siRNA (13). Following a recent analysis of ovarian cancer cell lines (26), we extended our analysis to a wider number of HGSC cell lines and confirmed consistent amplicon-dependent sensitivity to siRNA-mediated *CCNE1* and *CDK2* knockdown (Fig. 1A and Supplementary Fig. S1A and S1B). The OVCAR8 cell line has a low-level gain of *CCNE1* and was not sensitive to *CCNE1* or *CDK2* knockdown (Fig. 1A). However, OVCAR8 does not overexpress cyclin E1 at the mRNA or protein level (Supplementary Fig. S1B and S1C) compared with other cell lines such as OVCAR4 that have similar *CCNE1* copy number. These findings suggest a threshold of *CCNE1*/*CDK2* dependency that may be relevant to patient selection in clinical trials targeting this oncogene in HGSC.

To validate the effect of *CDK2* knockdown, we utilized a tetracycline-inducible shRNA targeting *CDK2* (Fig. 1B). Consistent with the siRNA data, inhibition of *CDK2* by shRNA resulted in reduced clonogenic survival, more evident in the *CCNE1*-amplified cell line, OVCAR3 compared with the *CCNE1*-unamplified cell line CAOV3 (Fig. 1C). Knockdown of *CDK2* was validated at the protein level (Supplementary Fig. S2A). Cell-cycle analysis demonstrated arrest in G_1, seen only in the OVCAR3 cell line (Fig. 1D). We did not observe significant levels of apoptosis following CDK2 knockdown, as assessed by percentage of Annexin V–positive cells measured by FACS (Supplementary Fig. S2B).

Cells transduced with CDK2-shRNA were grown as xenografts in NOD/SCID mice to examine the effects of *CDK2* knockdown *in vivo*. Consistent with the *in vitro* data, attenuation of *CDK2* expression in the OVCAR3 xenograft model resulted in significant tumor growth arrest in the group receiving doxycycline in food and water compared with controls (Fig. 1E–F). Induction of shRNA by doxycycline was monitored by *CDK2* gene expression measured by RT-PCR (Supplementary Fig. S2C). Reduced Rb1 phosphorylation was observed following *CDK2* knockdown in OVCAR3 tumors harvested at 7 days following induction (Fig. 1G), providing a biomarker of targeting cyclinE1/CDK2.

Taken together, *CCNE1*-amplified HGSC appear selectively sensitive to siRNA- and shRNA-mediated knockdown of *CDK2* both *in vitro* and *in vivo*. These findings support our previous studies and point to CDK2 as a potential therapeutic target in *CCNE1*-amplified HGSC.

CDK2 inhibitor dinaciclib delayed tumor growth in *CCNE1*-amplified HGSC xenografts

Consistent with siRNA data, we previously showed in a limited number of cell lines selective sensitivity of *CCNE1*-amplified cell lines to dinaciclib, a potent CDK2 inhibitor in advanced clinical development (13). However, in this study, when tested across a broader panel of HGSC cell lines, there did not appear to be a clear amplicon-dependent sensitivity (Fig. 2A), in contrast with the siRNA and shRNA data. Furthermore, activity *in vivo* was also seen in a xenograft model developed from a *CCNE1*-unamplified cell line, CAOV3 (Fig. 2B–D). The difference in amplicon-dependent sensitivity between gene suppression and pharmacologic inhibition may be due to the broad activity of dinaciclib, which, in addition to inhibiting CDK2, is also active against CDK1, 5, 9, and 12 (17, 27).

In addition to CDK2 inhibitors, we previously identified use of bortezomib, a proteasome inhibitor, as a potential therapeutic strategy for *CCNE1*-amplified HGSC (12). Although we did not observe amplicon-dependent sensitivity to dinaciclib, we investigated the interaction between dinaciclib and bortezomib to see whether the two drugs would be synergistic in combination. Using the Chou–Talalay methodology for drug combination studies (28), we did not observe a synergistic interaction with dinaciclib and bortezomib (Fig. 2E and F) in a panel of *CCNE1*-amplified and *CCNE1*-unamplified HGSC cell lines. Given this lack of synergism, we sought to identify selective synergistic drug combinations by adopting an unbiased high-throughput screening approach.

A high-throughput compound screen identifies synergistic drug combinations

We performed a high-throughput compound screen to identify combinations that would be synergistic in *CCNE1*-amplified cells, as well as combinations that would be selective in a CDK inhibitor–resistant cell line OVCAR3-R1-533533 (13). In the primary screen, 4,059 compounds (including duplicates) were combined with a fixed dose of dinaciclib as described in Materials and Methods. Dose–response curves were generated and manually curated, and compounds where a curve could not be fitted were excluded from the analysis. A full list of EC_{50} values for each cell line and compound is given in Supplementary Tables S4 and S5.

EC_{50} values from the primary screen were used to make two pair-wise comparisons (Fig. 2G and H): (i) dinaciclib plus library compound comparing OVCAR3 (*CCNE1*-amplified) versus SKOV3 (*CCNE1*-unamplified) and (ii) dinaciclib plus library compound comparing OVCAR3 (parental) and OVCAR3-R1 (CDK inhibitor resistant). At the time of undertaking the screen, SKOV3 was a commonly used ovarian cancer cell line; however, recent studies have demonstrated that SKOV3 is unlikely to resemble HGSC (26). Therefore, any potential hits identified in the screen were subsequently validated using only HGSC cell lines.

Library compounds where the ratio of EC_{50} was less than 0.5 were selected as hits for a secondary screen involving a total of 64 compounds (Supplementary Table S6 and S7). Compounds that

(*Continued.*) $n = 3$. **C,** HGSC cell lines were cultured *in vitro* with dinaciclib, MK-2206, or the combination for 24 hours and then analyzed using flow cytometry for Annexin V/propidium iodide positivity. Bars, mean ± SEM, $n = 3$. *, $P < 0.05$; **, $P < 0.01$; ***, $P < 0.001$; unpaired *t* test. **D,** *In vivo* effects of vehicle, dinaciclib, MK-2206, or combination. Immunocompromised mice bearing OVCAR3 (*CCNE1*-amplified) or CAOV3 (*CCNE1*-unamplified) tumor xenografts were treated with vehicle or drug as described in Materials and Methods. Plots represent mean tumor volume change from baseline ± SEM, $n = 5$ mice per group. **E,** Percentage tumor growth inhibition following 21 days of treatment with vehicle, dinaciclib, MK-2206, or the combination. Bars, mean ± SEM, $n = 5$ mice per group. Statistical analysis performed with ANOVA followed by Dunnett *post hoc* test to compare the percentage tumor growth inhibition between the treatment groups. *, $P < 0.05$; **, $P < 0.01$; ****, $P < 0.0001$. **F,** Quantitation of immunohistochemical staining for Ki67 and cleaved caspase-3. Bars, mean percentage of Ki67 or cleaved caspase-3–positive cells relative to background number of cells measured ± SEM, $n = 3$ in each group. Statistical analysis performed by ANOVA with Tukey multiple comparison test to compare between treatment groups. **G,** Subcutaneous tumors were obtained after 24 hours of treatment and were examined by IHC for biomarker analysis. Rb phosphorylation was inhibited by dinaciclib, but not MK-2206 treatment. AKT phosphorylation was inhibited by MK-2206, but not dinaciclib treatment. Proliferation (Ki67) was inhibited and apoptosis (cleaved caspase-3) was induced by the combination of dinaciclib and MK-2206 in *CCNE1*-amplified xenograft model (OVCAR3).

Published OnlineFirst September 23, 2016; DOI: 10.1158/1078-0432.CCR-16-0620

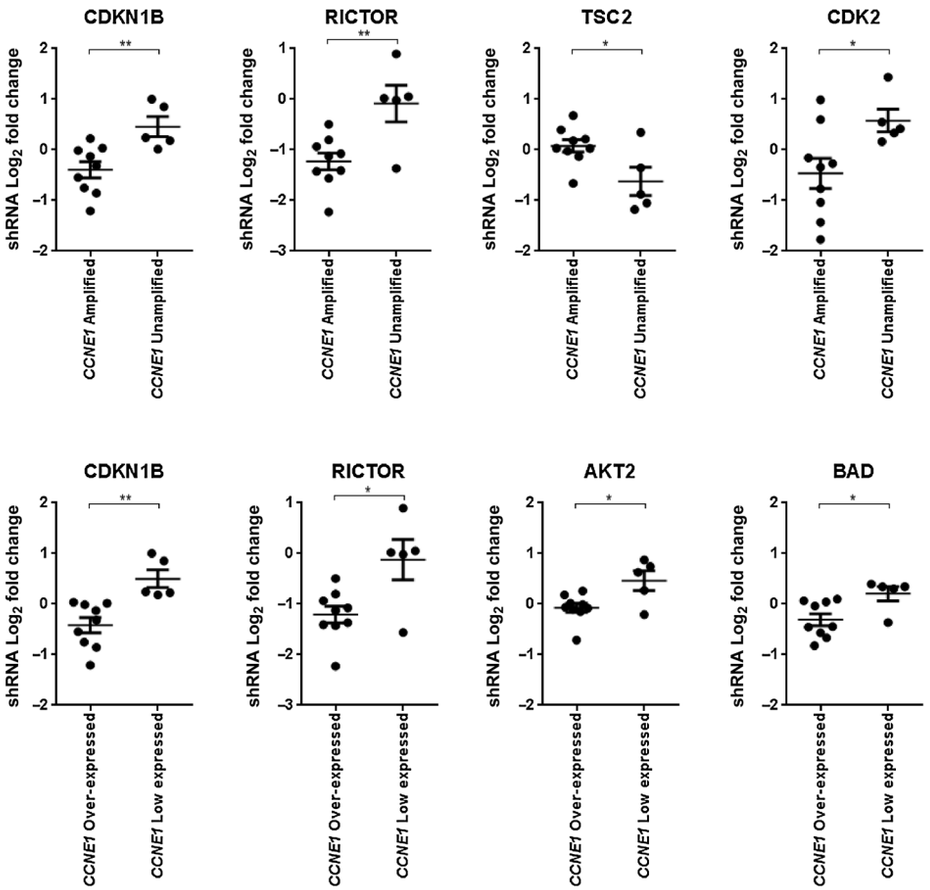

Figure 5.

CCNE1 and *AKT2* are coamplified in primary HGSC samples. Dot plots of median shRNA abundance for each gene targeted by shRNA in HGSC cell lines, stratified by *CCNE1* copy number or expression. Depletion of shRNA abundance within a group suggests requirement for maintained expression of its target gene. Only genes with a statistically significant difference are shown; see Supplementary Table S3 for the list of genes and cell lines analyzed. Statistical significance (*t* test) calculated by comparison between *CCNE1*-amplified and unamplified or *CCNE1* overexpressing and low expressing cell lines; *, $P < 0.05$; **, $P < 0.01$.

appeared to have an additive effect with dinaciclib were selected as hits from the secondary screen and carried forward for further testing.

The final part of the screen involved assessing the level of synergy between the library compound hits and dinaciclib involving an 11-point titration of each compound. Using the Chou–Talalay methodology of constant-ratio drug combinations, a series of combination indexes were generated to identify synergistic interactions.

In the OVCAR3 parental cell line, there were no synergistic combinations identified between dinaciclib and the library compounds (Supplementary Table S8). In the OVCAR3-R1 cell line, there were a number of synergistic interactions identified (Supplementary Table S8). Nonselective BH3-mimetic agents ABT-263 and ABT-737 were synergistic in combination with dinaciclib, suggestive of a class effect. This was validated further in an independently derived dinaciclib-resistant cell line, OVCAR3-RD6 (Fig. 3A–B and Supplementary Fig. S4A–S4C). There was no synergistic interaction noted in the combination between dinaciclib and ABT-199 (Fig. 3C), a selective Bcl-2 antagonist. The combination of dinaciclib and ABT-737 resulted in a dose-dependent increase in apoptosis, observed only in CDK inhibitor–resistant cell lines as demonstrated by increase in PARP cleavage products on Western blot analysis (Fig. 3D). Mcl-1 protein expression was not observed in the OVCAR3-RD6 cell line resistant to dinaciclib (Fig. 3D). Real-time PCR demonstrated upregulation of antiapoptotic genes in the dinaciclib and PHA533533-resistant cell lines (Fig. 3E), but downregulation of *MCL1* in the dinaciclib-resistant OVCAR3-RD cell lines. Dinaciclib is reported to have a greater effect on CDK9 compared with PHA533533 (13). Given that *MCL1* is regulated by CDK9 activity (29), this may explain the reduction of *MCL1* levels in the presence of dinaciclib. However, it is unclear why reduced *MCL1* expression is also apparent in OVCAR3-RD cell lines even when grown in the absence of dinaciclib.

MK-2206, a pan-AKT inhibitor, was identified as a synergistic drug combination in the CDK inhibitor–resistant cell line, OVCAR3-R1. In validating this interaction between dinaciclib and MK-2206, we observed that this combination was also synergistic in *CCNE1*-amplified cell lines FUOV1 and parental OVCAR3 (Fig. 4A). This effect was similarly observed with another AKT inhibitor, GSK-2110183 (Fig. 4B), that was not included in the original high-throughput screen library. Exposure to dinaciclib and MK2206 resulted in significantly higher number of apoptotic cells in *CCNE1*-amplified cell lines, indicated by percentage of Annexin V–positive cells measured by FACS (Fig. 4C). This result was similarly observed on Western blot analysis, with appearance of PARP cleavage products following treatment of OVCAR3 cells with the combination of dinaciclib and MK-2206 (Supplementary Fig. S4D). As dinaciclib targets several CDKs in addition to CDK2 (17), we used siRNA knockdown of CDK2, CDK1, or CDK9 to determine the specificity of the synergistic effect of dinaciclib and MK-2206. We found that the synergy observed was predominantly mediated through CDK2 (Supplementary Fig. S4E).

Published OnlineFirst September 23, 2016; DOI: 10.1158/1078-0432.CCR-16-0620

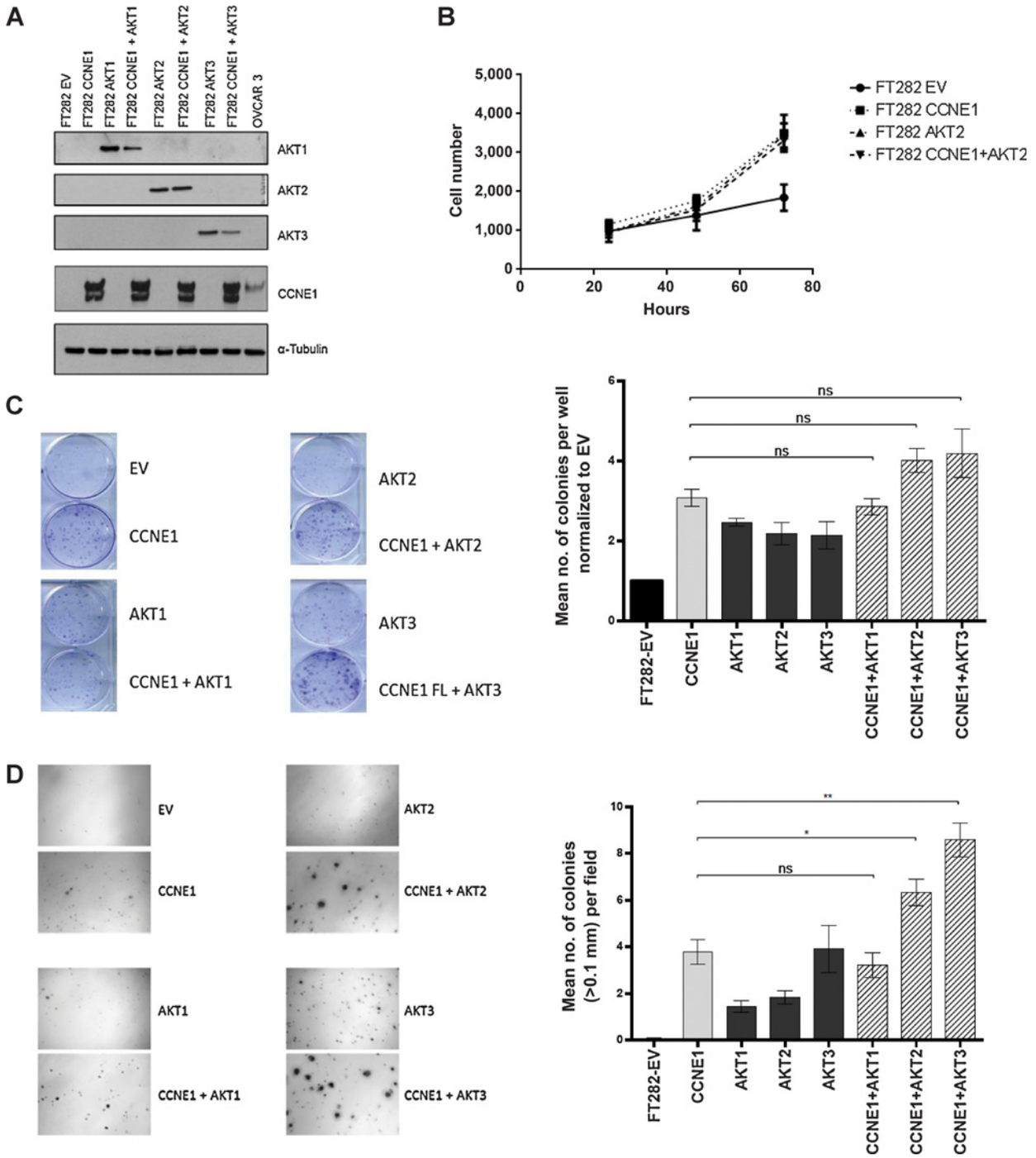

Figure 6.

Cyclin E1 and AKT overexpression cooperates to promote uncontrolled growth in FTSECs. **A,** Western blot analysis of fallopian tube secretory cells transduced with cyclin E1, empty vector, and AKT1, AKT2, and AKT3 overexpression constructs. Blots are representative of three independently performed experiments. **B,** Proliferation assay of fallopian tube secretory cells (FT282) transduced with empty vector (EV), cyclin E1 (CCNE1), AKT2, and both cyclin E1 and AKT2 (CCNE1+AKT2). Plots represent mean of three independently performed experiments, error bars represent SEM. **C,** Clonogenic survival assay of FT282 cells transduced as labeled. Images (left) show cells fixed and stained with crystal violet. Bar chart represents mean of three independently performed experiments, error bars represent SEM. Statistical significance (*t* test) calculated by comparison with FT282 cells transduced with cyclin E1 (FT282-CCNE1). **D,** Anchorage-independent assay of FT282 cells transduced as labeled. Images (left) represent cells fixed with 2% paraformaldehyde and captured using an Olympus IX81 live cell imager. Bar chart represents mean of three independently performed experiments, error bars represent SEM. Statistical significance (*t* test) calculated by comparison with FT282 cells transduced with cyclin E1 (FT282-CCNE1); *, $P < 0.05$, **, $P < 0.01$.

Published OnlineFirst September 23, 2016; DOI: 10.1158/1078-0432.CCR-16-0620

Dinaciclib and MK-2206 are selectively synergistic in *CCNE1*-amplified cell lines *in vivo*

The *in vivo* effect of dinaciclib and MK-2206 was assessed using xenograft models from *CCNE1*-amplified and unamplified cell lines, OVCAR3 and CAOV3, respectively. The combination was significantly more effective than each single agent alone in the *CCNE1*-amplified model (Fig. 4D and E), whereas there was no statistically significant effect of the combination compared to single-agent treatment in the *CCNE1*-unamplified model. After a treatment period of three weeks with dinaciclib and MK-2206, xenograft tumors began regrowing within 10 days of treatment cessation. Rechallenge with the same drug combination resulted in significant tumor regression (Supplementary Fig. S4F), indicating continued sensitivity to the combination. Consistent with this effect on tumor growth, treatment with dinaciclib and MK-2206 resulted in inhibition of cell proliferation and induction of apoptosis, as assessed by Ki67 and cleaved caspase-3 IHC on tumors harvested at 24 hours (Fig. 4F and G). Taken together, the high-throughput screen identified a novel combination of dinaciclib and MK-2206 that appeared to be selectively synergistic in *CCNE1*-amplified HGSC cell lines both *in vitro* and *in vivo*.

***CCNE1* and *AKT2* are frequently coamplified in primary HGSC samples**

We sought to investigate whether there was evidence for an interaction between *CCNE1* amplification and the AKT pathway in primary tumor samples. Analysis of TCGA dataset indicated that *CCNE1* and *AKT2* amplification events cooccur ($P < 0.001$; Supplementary Fig. S5). This observation was not seen with other isoforms of AKT or genes in the AKT pathway. To examine the relationship between *CCNE1* amplification and the AKT pathway further, we made use of data from Project Achilles, a genome-wide shRNA screen of synthetic lethality in 216 cancer cell lines (24). The abundance of shRNA sequence relative to a reference pool was measured by microarray to identify genes essential for survival. We analyzed the effect of shRNA-targeting genes within the AKT pathway, restricting the analysis to HGSC cell lines, classified according to *CCNE1* copy number or expression. A statistically significant dependence on genes in the AKT pathway, including *AKT2*, was observed, indicated by a depletion of shRNAs targeting these genes in cell lines with *CCNE1* amplification or overexpression (Fig. 5). *CDK2* was included in the analysis as a control, and consistent with our previous analysis, was shown to be required in *CCNE1*-amplified cells (13).

Cyclin E1 and AKT overexpression cooperates to promote uncontrolled growth in FTSECs

Previously, Karst and colleagues demonstrated that cyclin E1 overexpression combined with *TP53* mutation in FTSECs resulted in increased proliferation, colony-forming ability, and colony formation in soft agar (19). However, cyclin E1 overexpression alone did not result in complete transformation, suggesting that additional events are required.

We examined the interaction between cyclin E1 and AKT overexpression in FTSECs by overexpressing the myristoylated, active forms of AKT1, AKT2, and AKT3 (20). Expression of each AKT isoform and cyclin E1 was validated with Western blot analysis (Fig. 6A) and RT-PCR (Supplementary Fig. S6A). Overexpression of AKT isoforms led to increased expression of AKT downstream targets (Supplementary Fig. S6B). AKT2 and cyclin E1 overexpression alone or in combination showed a trend toward increased proliferation compared with empty vector alone (Fig. 6B), and AKT2 or AKT3 overexpression in combination with cyclin E1 showed a trend toward enhanced clonogenic colony formation in comparison with overexpression of cyclin E1 alone (Fig. 6C). There was a significant increase in soft agar colony formation with the overexpression of AKT2 or AKT3 in combination with cyclin E1 compared with overexpression of cyclin E1 alone (Fig. 6D). These findings support an interaction between cyclin E1 and AKT pathway to promote uncontrolled growth in FTSECs, and may explain synergism observed between dinaciclib and MK-2206 in *CCNE1*-amplified HGSC.

Discussion

HGSC patients with *CCNE1* amplification have a clear unmet need in terms of effective therapies. In this study, we validate *CDK2* as a selective target in *CCNE1*-amplified HGSC using shRNA-mediated gene suppression *in vitro* and *in vivo*. However, we did not observe similar amplicon-dependent specificity to dinaciclib, a small-molecule inhibitor targeting CDKs. This may be due to the nonspecificity of inhibitors such as dinaciclib or a role for kinase-independent activities of *CCNE1* in amplified HGSC (30). Our findings highlight the potential differences between inhibition of kinase activity and complete suppression of *CCNE1* or *CDK2* gene expression.

In addition to CDK2, dinaciclib targets CDK1, 5, 9, and 12 (17, 27). CDK9 phosphorylates the carboxyl-terminal repeat domains of RNA polymerase II, and inhibition of CDK9 by dinaciclib results in rapid downregulation of mRNA transcripts and proteins with short half-lives such as the antiapoptotic BCL2 family member, Mcl1 (17). Preclinical studies have indicated dinaciclib-mediated targeting of Mcl-1 may be an effective therapeutic approach in a number of different cancers (17). Inhibition of CDK2 kinase activity may also differ significantly from complete suppression of gene expression, resulting in varying downstream and compensatory effects (31, 32). Studies with knockout experiments indicate that CDK2 functions appear redundant with CDK1, although in our studies, we did not observe upregulation of CDK1 expression following CDK2 knockdown *in vitro* or *in vivo* (data not shown).

Although we observed a difference in the amplicon-dependent sensitivity of *CDK2* gene suppression compared with pharmacologic inhibition, dinaciclib remains a potent CDK2 inhibitor with single-agent activity in *CCNE1*-amplified HGSC cell lines and is one of the most clinically advanced CDK2 inhibitors (33). Therefore, to more effectively target *CCNE1*-amplified HGSCs, we performed a combinatorial drug screen to identify compounds that would synergize with dinaciclib. We also sought to identify compounds that may potentially overcome resistance to dinaciclib, a common occurrence in the clinical use of targeted small-molecule inhibitors, by testing a cell line that was resistant to CDK inhibitors. Dinaciclib in combination with MK-2206, an AKT inhibitor, was identified as a synergistic combination in targeting CDK inhibitor–resistant cell lines. This supported our previous work that identified increased *AKT1* copy number and upregulation of genes in the AKT pathway as a potential mechanism of resistance to CDK2 inhibitors (13). In validating this finding, we observed selective, potent synergism between dinaciclib and MK-2206 *in vitro* and *in vivo* models of *CCNE1*-amplified HGSCs, including parental OVCAR3 cells. This interaction was not initially observed in the primary high-throughput screen. However,

Published OnlineFirst September 23, 2016; DOI: 10.1158/1078-0432.CCR-16-0620

the use of SKOV3 cell line as a comparator in the screen may be a potential confounder, as the selection of compounds as hits from the primary screen was based on a difference in the EC_{50} values between the two cell lines tested, OVCAR3 and SKOV3. Recently, multiple studies characterizing the genomic profile of commercially available ovarian cancer cell lines have shown that many of these cell lines, including SKOV3, may not accurately resemble HGSC (26, 34–36).

Synergism between dinaciclib and MK-2206, as well as another AKT-specific inhibitor GSK2110183, but an absence of a synergistic combination with other inhibitors of the PI3K–AKT–mTOR pathway suggests that the interaction with *CCNE1* may be specific to AKT. Analysis of genomic data from patients demonstrated a significant cooccurrence of *CCNE1* and *AKT2* amplification, which may in part be explained by colocalization on chromosome 19q. However, FUOV1, which has *CCNE1*-amplification without *AKT2*-amplification (25), was equally sensitive to the combination of dinaciclib and AKT inhibitors. Coexpression of AKT2 or AKT3 with cyclin E1 in a *TP53*-mutant FTSEC cell line resulted in increased proliferation and anchorage-independent growth. Analysis of data from Project Achilles indicates that HGSC cell lines that have *CCNE1* amplification or overexpression are dependent on multiple genes within the AKT pathway. We previously performed a pathway analysis of genes coexpressed with *CCNE1* amplification and observed an enrichment of genes involved in AKT signaling (12). Collectively, these data suggest a specific dependency of *CCNE1*-amplified tumors for AKT activity.

Dinaciclib and MK-2206 have previously been shown to be active against pancreatic adenocarcinoma (37). In *KRAS*-mutant pancreatic cancer patient–derived xenografts, Hu and colleagues (37) demonstrated efficacy of dinaciclib combined with MK-2206. They proposed that sensitivity was due to the effect of dinaciclib on CDK5, and in turn, inhibition of RAL pathway. On the basis of these results, a phase I clinical trial (NIH Trial NCT01783171) of dinaciclib and MK-2206 has been initiated in patients with advanced pancreatic cancer. While this trial will provide safety and recommended dosing of the combination, patients are not preselected on the basis of tumoral *CCNE1* amplification, and the mechanism of interaction and biomarkers that predict response are likely to be different in pancreatic cancer compared with HGSC.

Other combinations were also identified from the high-throughput screen. In particular, nonselective BH3-mimetic compounds ABT-737 and ABT-263 were synergistic in combination with dinaciclib in CDK inhibitor–resistant cell lines. There was no synergistic interaction between dinaciclib and the Bcl-2–specific antagonist, ABT-199, indicating that the targeting of multiple antiapoptotic proteins is potentially required to overcome resistance to CDK2 inhibitors. This observation is supported by upregulation of multiple genes in this pathway including BCL-2, BCL-XL, and BCL-W in resistant cell lines. However, the use of ABT-737 or ABT-263 in combination with dinaciclib *in vivo* is hindered by significant toxicities, particularly hematologic (Joel Leverson, personal communication), and are therefore unlikely to have clinical utility.

Biomarker-driven trials in HGSC are needed to improve clinical outcomes. HGSC patients with *CCNE1* amplification are a subset that requires different treatment approaches, given that they have HR-proficient tumors, and as such, are likely to have poor responses to platinum-based chemotherapy and PARP inhibitors. However, targeted therapies when used alone may not be sufficient to induce selective, cytotoxic effects, and often result in the development of resistance. Combination therapies may potentially be a strategy to overcome these limitations. High-throughput drug screening is an unbiased approach to identify novel therapeutic strategies, and we have identified dinaciclib and MK-2206 as a combination that may prove to selectively target patients with *CCNE1*-amplified HGSC. Further work incorporating additional clinically relevant models and novel combinations will inform the design of rational clinical trials targeting *CCNE1*-amplified HGSC.

Disclosure of Potential Conflicts of Interest

No potential conflicts of interest were disclosed.

Authors' Contributions

Conception and design: G. Au-Yeung, W.J. Azar, C. Cullinane, D. Rischin, R. Drapkin, D. Etemadmoghadam, D.D.L. Bowtell

Development of methodology: G. Au-Yeung, F. Lang, W.J. Azar, K. Lackovic, R.B. Pearson, R. Drapkin

Acquisition of data (provided animals, acquired and managed patients, provided facilities, etc.): G. Au-Yeung, F. Lang, W.J. Azar, K.E. Jarman, K. Lackovic, D. Aziz

Analysis and interpretation of data (e.g., statistical analysis, biostatistics, computational analysis): G. Au-Yeung, F. Lang, W.J. Azar, K. Lackovic, C. Cullinane, D.D.L. Bowtell

Writing, review, and/or revision of the manuscript: G. Au-Yeung, F. Lang, C. Mitchell, K. Lackovic, C. Cullinane, R.B. Pearson, L. Mileshkin, D. Rischin, D. Etemadmoghadam, D.D.L. Bowtell

Administrative, technical, or material support (i.e., reporting or organizing data, constructing databases): W.J. Azar, C. Mitchell, K.E. Jarman, R. Drapkin

Study supervision: L. Mileshkin, D. Rischin, D. Etemadmoghadam, D.D.L. Bowtell

Other [created material integral to the study (engineered primary human cell lines)]: A.M. Karst

Acknowledgments

The authors wish to acknowledge staff from the Peter MacCallum Cancer Centre Animal facility, FACS facility, and Histology core facility for their assistance.

Grant Support

This work was supported by a National Health and Medical Research Council (NHMRC) program grant (APP1092856; to D.D.L. Bowtell), NHMRC project grant (APP1042358; to D. Etemadmoghadam), a Pfizer Cancer Research Grant (WI80176; to G. Au-Yeung), University of Melbourne Australian Postgraduate Award (to G. Au-Yeung), the U.S. Army Medical Research and Materiel Command (OC140511; to D.D.L. Bowtell and R. Drapkin), the National Cancer Institute at the NIH (P50-CA083636 and R21 CA156021; to R. Drapkin); the Honorable Tina Brozman ˜Tina's Wish' Foundation (to R. Drapkin), the Dr. Miriam and Sheldon G. Adelson Medical Research Foundation (to R. Drapkin), a Canadian Institutes of Health Research Fellowship (to A.M. Karst), a Kaleidoscope of Hope Foundation Young Investigator Research grant (to A.M. Karst), the Basser Center for BRCA, and Department of Obstetrics and Gynecology at the University of Pennsylvania Perelman School of Medicine (to R. Drapkin). The Australian Ovarian Cancer Study is supported by the Peter MacCallum Cancer Centre Foundation, U.S. Army Medical Research and Materiel Command under DAMD17-01-1-0729, The Cancer Council Victoria, Queensland Cancer Fund, The Cancer Council New South Wales, The Cancer Council South Australia, The Cancer Foundation of Western Australia, The Cancer Council Tasmania, and the National Health and Medical Research Council of Australia (NHMRC; ID#628779), Stephanie Boldeman, the Agar family, and Ovarian Cancer Australia.

The costs of publication of this article were defrayed in part by the payment of page charges. This article must therefore be hereby marked *advertisement* in accordance with 18 U.S.C. Section 1734 solely to indicate this fact.

Received March 10, 2016; revised September 6, 2016; accepted September 12, 2016; published OnlineFirst September 23, 2016.

Published OnlineFirst September 23, 2016; DOI: 10.1158/1078-0432.CCR-16-0620

References

1. Martini M, Vecchione L, Siena S, Tejpar S, Bardelli A. Targeted therapies: how personal should we go? Nat Rev Clin Oncol 2012;9:87–97.
2. Burger RA, Brady MF, Bookman MA, Fleming GF, Monk BJ, Huang H, et al. Incorporation of bevacizumab in the primary treatment of ovarian cancer. N Engl J Med 2011;365:2473–83.
3. Perren TJ, Swart AM, Pfisterer J, Ledermann JA, Pujade-Lauraine E, Kristensen G, et al. A phase 3 trial of bevacizumab in ovarian cancer. N Engl J Med 2011;365:2484–96.
4. Fong PC, Boss DS, Yap TA, Tutt A, Wu P, Mergui-Roelvink M, et al. Inhibition of poly(ADP-ribose) polymerase in tumors from BRCA mutation carriers. N Engl J Med 2009;361:123–34.
5. Ledermann J, Harter P, Gourley C, Friedlander M, Vergote I, Rustin G, et al. Olaparib maintenance therapy in platinum-sensitive relapsed ovarian cancer. N Engl J Med 2012;366:1382–92.
6. Ahmed AA, Etemadmoghadam D, Temple J, Lynch AG, Riad M, Sharma R, et al. Driver mutations in TP53 are ubiquitous in high grade serous carcinoma of the ovary. J Pathol 2010;221:49–56.
7. Cancer Genome Atlas Research Network. Integrated genomic analyses of ovarian carcinoma. Nature 2011;474:609–15.
8. Patch AM, Christie EL, Etemadmoghadam D, Garsed DW, George J, Fereday S, et al. Whole-genome characterization of chemoresistant ovarian cancer. Nature 2015;521:489–94.
9. Scott CL, Swisher EM, Kaufmann SH. Poly (ADP-ribose) polymerase inhibitors: recent advances and future development. J Clin Oncol 2015;33:1397–406.
10. Etemadmoghadam D, deFazio A, Beroukhim R, Mermel C, George J, Getz G, et al. Integrated genome-wide DNA copy number and expression analysis identifies distinct mechanisms of primary chemoresistance in ovarian carcinomas. Clin Cancer Res 2009;15:1417–27.
11. Nakayama N, Nakayama K, Shamima Y, Ishikawa M, Katagiri A, Iida K, et al. Gene amplification CCNE1 is related to poor survival and potential therapeutic target in ovarian cancer. Cancer 2010;116:2621–34.
12. Etemadmoghadam D, Weir BA, Au-Yeung G, Alsop K, Mitchell G, George J, et al. Synthetic lethality between CCNE1 amplification and loss of BRCA1. Proc Natl Acad Sci U S A 2013;110:19489–94.
13. Etemadmoghadam D, Au-Yeung G, Wall M, Mitchell C, Kansara M, Loehrer E, et al. Resistance to CDK2 inhibitors is associated with selection of polyploid cells in CCNE1-amplified ovarian cancer. Clin Cancer Res 2013;19:5960–71.
14. Ellis LM, Hicklin DJ. Resistance to targeted therapies: refining anticancer therapy in the era of molecular oncology. Clin Cancer Res 2009;15:7471–8.
15. Yap TA, Omlin A, de Bono JS. Development of therapeutic combinations targeting major cancer signaling pathways. J Clin Oncol 2013;31:1592–605.
16. Fitzgerald JB, Schoeberl B, Nielsen UB, Sorger PK. Systems biology and combination therapy in the quest for clinical efficacy. Nat Chem Biol 2006;2:458–66.
17. Parry D, Guzi T, Shanahan F, Davis N, Prabhavalkar D, Wiswell D, et al. Dinaciclib (SCH 727965), a novel and potent cyclin-dependent kinase inhibitor. Mol Cancer Ther 2010;9:2344–53.
18. Fellmann C, Hoffmann T, Sridhar V, Hopfgartner B, Muhar M, Roth M, et al. An optimized microRNA backbone for effective single-copy RNAi. Cell Rep 2013;5:1704–13.
19. Karst AM, Jones PM, Vena N, Ligon AH, Liu JF, Hirsch MS, et al. Cyclin E1 deregulation occurs early in secretory cell transformation to promote formation of fallopian tube-derived high-grade serous ovarian cancers. Cancer Res 2014;74:1141–52.
20. Astle MV, Hannan KM, Ng PY, Lee RS, George AJ, Hsu AK, et al. AKT induces senescence in human cells via mTORC1 and p53 in the absence of DNA damage: implications for targeting mTOR during malignancy. Oncogene 2012;31:1949–62.
21. Lackovic K, Lessene G, Falk H, Leuchowius KJ, Baell J, Street I. A perspective on 10-years HTS experience at the walter and eliza hall institute of medical research - eighteen million assays and counting. Comb Chem High Throughput Screen 2014;17:241–52.
22. Cerami E, Gao J, Dogrusoz U, Gross BE, Sumer SO, Aksoy BA, et al. The cBio cancer genomics portal: an open platform for exploring multidimensional cancer genomics data. Cancer Discov 2012;2:401–4.
23. Gao J, Aksoy BA, Dogrusoz U, Dresdner G, Gross B, Sumer SO, et al. Integrative analysis of complex cancer genomics and clinical profiles using the cBioPortal. Sci Signal 2013;6:pl1.
24. Cowley GS, Weir BA, Vazquez F, Tamayo P, Scott JA, Rusin S, et al. Parallel genome-scale loss of function screens in 216 cancer cell lines for the identification of context-specific genetic dependencies. Sci Data 2014;1:140035.
25. Barretina J, Caponigro G, Stransky N, Venkatesan K, Margolin AA, Kim S, et al. The cancer cell line encyclopedia enables predictive modelling of anticancer drug sensitivity. Nature 2012;483:603–7.
26. Domcke S, Sinha R, Levine DA, Sander C, Schultz N. Evaluating cell lines as tumour models by comparison of genomic profiles. Nat Commun 2013;4:2126.
27. Shapiro G. Beyond CDK4/6: Targeting additional cell cycle and transcriptional CDKs in breast cancer [abstract]. In: Proceedings of the Thirty-Eighth Annual CTRC-AACR San Antonio Breast Cancer Symposium; 2015 Dec 8–12; San Antonio, TX. Philadelphia (PA): AACR. Abstract nr MS1–1.
28. Chou TC. Drug combination studies and their synergy quantification using the Chou-Talalay method. Cancer Res 2010;70:440–6.
29. Gojo I, Zhang B, Fenton RG. The cyclin-dependent kinase inhibitor flavopiridol induces apoptosis in multiple myeloma cells through transcriptional repression and down-regulation of Mcl-1. Clin Cancer Res 2002;8:3527–38.
30. Geng Y, Lee YM, Welcker M, Swanger J, Zagozdzon A, Winer JD, et al. Kinase-independent function of cyclin E. Mol Cell 2007;25:127–39.
31. Horiuchi D, Huskey NE, Kusdra L, Wohlbold L, Merrick KA, Zhang C, et al. Chemical-genetic analysis of cyclin dependent kinase 2 function reveals an important role in cellular transformation by multiple oncogenic pathways. Proc Natl Acad Sci U S A 2012;109:E1019–27.
32. Echalier A, Cot E, Camasses A, Hodimont E, Hoh F, Jay P, et al. An integrated chemical biology approach provides insight into Cdk2 functional redundancy and inhibitor sensitivity. Chem Biol 2012;19:1028–40.
33. Asghar U, Witkiewicz AK, Turner NC, Knudsen ES. The history and future of targeting cyclin-dependent kinases in cancer therapy. Nat Rev Drug Discov 2015;14:130–46.
34. Anglesio MS, Wiegand KC, Melnyk N, Chow C, Salamanca C, Prentice LM, et al. Type-specific cell line models for type-specific ovarian cancer research. PLoS ONE 2013;8:e72162.
35. Beaufort CM, Helmijr JC, Piskorz AM, Hoogstraat M, Ruigrok-Ritstier K, Besselink N, et al. Ovarian cancer cell line panel (OCCP): clinical importance of *invitro* morphological subtypes. PLoS ONE 2014;9:e103988.
36. Elias KM, Emori MM, Papp E, MacDuffie E, Konecny GE, Velculescu VE, et al. Beyond genomics: critical evaluation of cell line utility for ovarian cancer research. Gynecol Oncol 2015;139:97–103.
37. Hu C, Dadon T, Chenna V, Yabuuchi S, Bannerji R, Booher R, et al. Combined inhibition of cyclin-dependent kinases (Dinaciclib) and AKT (MK-2206) blocks pancreatic tumor growth and metastases in patient-derived xenograft models. Mol Cancer Ther 2015;14:1532–9.

Published OnlineFirst September 23, 2016; DOI: 10.1158/1078-0432.CCR-16-0620

Clinical Cancer Research

Selective Targeting of Cyclin E1-Amplified High-Grade Serous Ovarian Cancer by Cyclin-Dependent Kinase 2 and AKT Inhibition

George Au-Yeung, Franziska Lang, Walid J. Azar, et al.

Clin Cancer Res 2017;23:1862-1874. Published OnlineFirst September 23, 2016.